Research on heat distribution design of carbon ceramic brake discs and shape optimization of rib for high-speed train

Yili Zhou, Shuguang Yao
Central South University

Abstract: High speed and lightweight are the development trends of high-speed trains in the world. Air braking technology is the last line of defense to ensure the safety and reliability of trains. The complex working environment and huge braking power put forward higher requirements for brake disc configuration and material. Carbon-ceramic composite materials have the characteristics of large specific heat capacity, thermal shock resistance, lightweight and high temperature resistance, and are considered to be high-performance friction materials. By imitating the distribution of animal and plant nutrients transportation pipelines, a carbon-ceramic composite brake disc structure with #-shaped heat dissipation ribs was designed that take into account the anisotropy of the thermal conductivity of carbon-ceramic composite materials. The branched rib structure realizes rapid heat transmission in the disc material, thereby achieving high efficiency and uniform temperature distribution, prevents the concentration of heat generated by friction, which can reduce the maximum temperature value under braking conditions. Then combined with the shape optimization and size optimization design of the local heat dissipation ribs of the brake disc. Further research on the uniform temperature performance and heat dissipation under emergency braking conditions of 400km/h was carried out. The LSR model was used to analyze the different outlet angle, inlet angle and number of the cooling ribs in the same reference flow field. By comprehensively considering parameters as the average maximum temperature, convection heat transfer coefficient, an optimal design that balances cooling efficiency and aerodynamic loss is obtained.

Keywords: High-speed train; Carbon ceramic brake disc; Thermal management; Shape optimization.

Introduction

Increasing brake disc energy and reducing disc weight are of great significance to speed up high-speed trains. Carbon/ceramic composite is a carbon fiber reinforced silicon carbide ceramic matrix composite. This new composite has low density (general less than 2.0g/cm^3), high temperature resistance (still has a high coefficient of friction and low wear rate at 1000℃) and other advantages [1,2]. However, problems such as excessively high temperature and large temperature gradient caused by emergency braking at higher speeds will cause damage to the brake disc and affect the final service life [3-6]. Therefore, by optimizing the structure design of the carbon ceramic composite brake disc, the transfer of heat

generated by friction in the disc structure and the heat exchange between the disc and the surrounding air can be changed. Maximize the use of material thermal properties and structural shape generated by convection heat transfer, to reduce the temperature of excessive and uneven damage.

Natural organisms constantly optimize themselves to adapt to environmental requirements. In order to ensure the development of normal physiological and metabolic functions, animal blood vessels and plant leaves have transmission channels that provide water and nutrients for animals and plants [7]. The brake disc friction ring can be regarded as a huge heat source input under the high-speed operation of the brake disc. The transmission channel concept formed by the long-term evolution of animals and plants is applied to the design of the brake disc heat sink plate structure. The heat in the brake disc friction ring is diffused through the bionic heat rib, and then dissipated by the heat convection, to solve the problem of temperature concentration caused by friction heat generation of brake disc.

1. Design of bionic cooling rib brake disc

All organs of the animal body are distributed with dense blood vessels, the distribution shape of blood vessels is shown in Fig. 1(a), where blood flows through the vessels. The nutrients absorbed by the digestive system and the oxygen of the respiratory system are transported to the whole body of the animal through the blood, which is required for the physiological activities of various tissues and cells in the body. The nutrient transport channel in the plant is shown in Fig. 1(b), the shape of this transport channel can realize the efficient transmission of nutrients in the plant and ensure the smooth progress of the normal physiological and metabolic functions of the leaves.

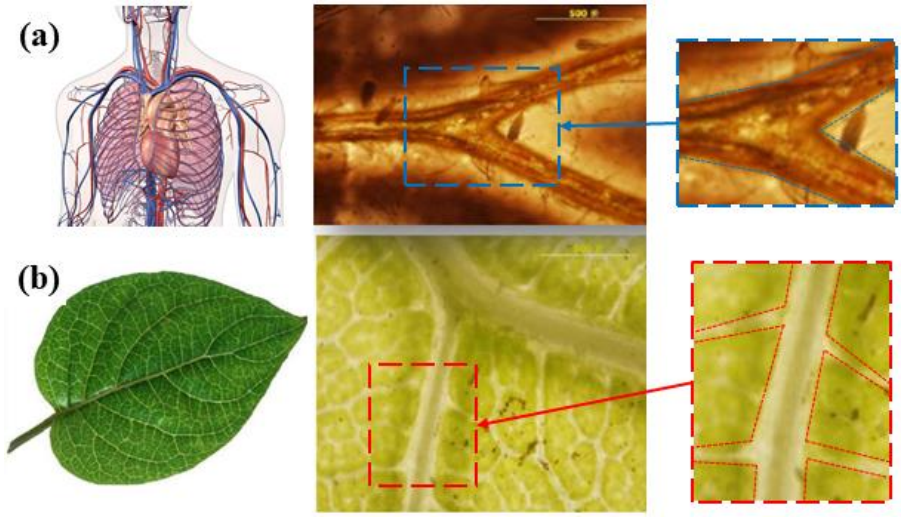

Fig. 1. Nutrient transport channels and channel amplification in animals and plants

Refer to nutrient transport channels in animals and plants, ventilated brake disc structure with three kinds of heat ribs as shown in Fig. 2. were established.

Based on this bionic concept, it can ensure that heat is transmitted to the heat dissipation layer through the efficient heat transfer function of the solid material, where the heat is generated by the high-speed thermal shock of the friction layer, then the heat is dissipated in the surrounding air through the convection heat transfer on the surface of the heat dissipation layer.

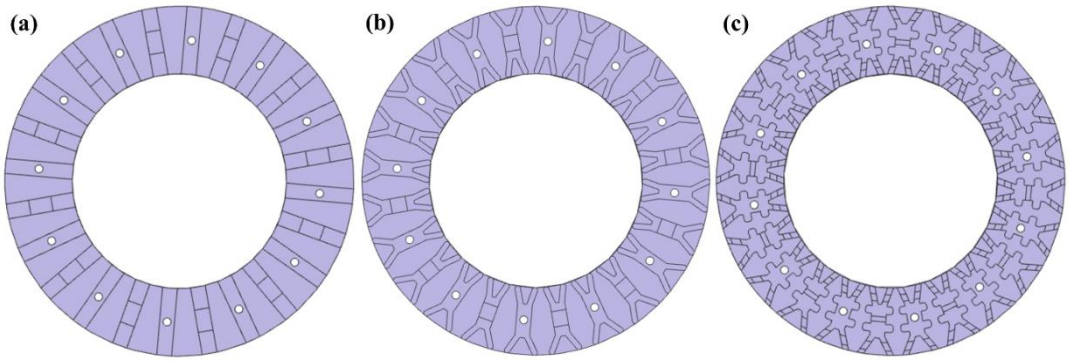

Fig. 2. Three bionic brake discs (a) Disc S; (a) Disc P; (a) Disc Z.

2. Geometric model

The heat dissipation ribs of the above shape are distributed at an interval of 15° on the surface of the support layer of the brake disc structure established. Bolt mounting holes are arranged on the separated heat dissipation ribs, and ventilation and heat dissipation grooves are designed at the corresponding positions of the bolt holes for the remaining heat dissipation ribs, as shown in Fig. 3(a). The thickness of the heat dissipation layer of the brake disc model is 26.5mm for t_1, the total thickness of the heat dissipation layer and the support layer is 46.5mm for t_2, and the inlet angle of the heat dissipation rib is φ and the outlet angle is θ. Ventilation slot width R_2-R_1 at the inner diameter is 15mm, ventilation slot width R_6-R_5 at the outermost diameter is 18mm, ventilation slot width R_4-R_3 at the middle position is 10mm, as shown in Fig. 3(b).

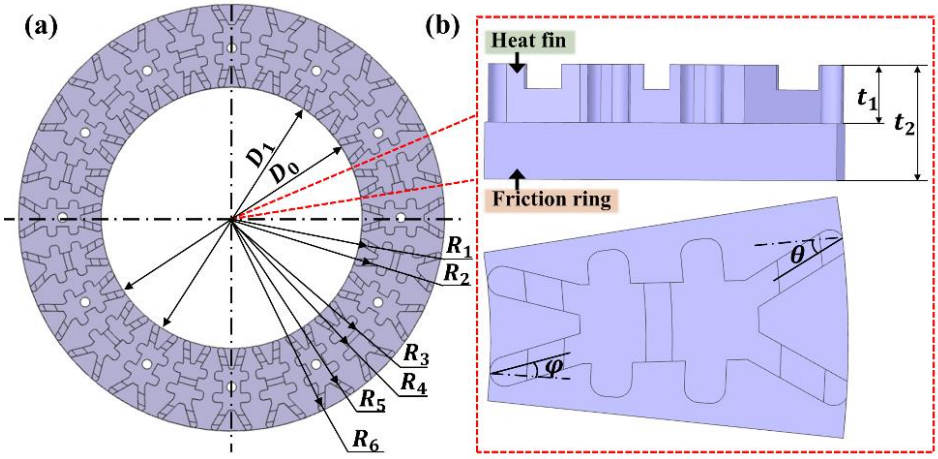

Fig. 3. The geometry of the brake disc. (a) Geometric shape;(b) Geometric details of the brake disc.

3. Numerical methods

3.1 Numerical model

The brake disc is made of carbon ceramic composite material, as shown in Table 1 [8,9]. During the braking process, due to the influence of many factors and conditions, the simulation conditions cannot be guaranteed to be consistent with the actual situation. In order to simplify the problem and make the results more convincing under the condition of ensuring the reliability of the solution results, the following assumptions are made:

(1) Only consider that the material properties of the brake disc of the brake are isotropic and homogeneous, and ignore the influence of temperature change on the mechanical properties of the material.

(2) The ambient temperature of the braking system during braking is 300K.

(3) Ignore the heat taken away by brake disc wear.

Emergency braking is one of the most severe braking conditions of high-speed train, which can make the train stop quickly in a short time. In the process of emergency braking, a small part of the heat on the ventilated brake disc is transferred to other parts such as the axle, and most of the heat is transferred to the heat sink through heat conduction, and is dissipated by the heat convection and heat radiation of the air.

Table 1 Thermophysical properties of carbon ceramic composite brake disc

Temperature (°C)	Specific heat capacity (J/(kg· K))	Density (kg/m^3)	Thermal conductivity (W/(m· K))	
			(∥)	(⊥)
30	1063	2300	81	57.6
100	1170		73.4	49.5
300	1642		61.7	45.7
500	2062		56.8	45.2
700	2590		55	46.5
900	2553		50.5	40
1100	2729		47.5	38.8
1300	2687		42.2	34

The thermal behavior of the brake disc and the interaction between the air flow around the brake disc and the thermal behavior of the brake disc were numerically simulated using the computational fluid dynamics analysis software ANSYS Fluent. The sliding grid is used to simulate the motion state of the flow field, the energy equation and heat radiation model are opened, and the Realizable turbulence model is selected to simulate the influence of air flow around the brake disc on the thermal behavior of the train during braking, as shown in Fig. 4. The inlet boundary condition is the velocity inlet condition, and the velocity direction is the positive direction of the X-axis. According to the study of influence of bogie

fairing on aerodynamic resistance, underbody flow characteristics, velocity and pressure distribution in the wake by Wang et al, the most dangerous calculation condition is taken and the inlet speed of the brake disc analysis model is set as 0.1 times the train running speed [4]. The pressure of the pressure outlet is 0Pa, the temperature is set to 300K, and the wall is set to no slip on the wall.

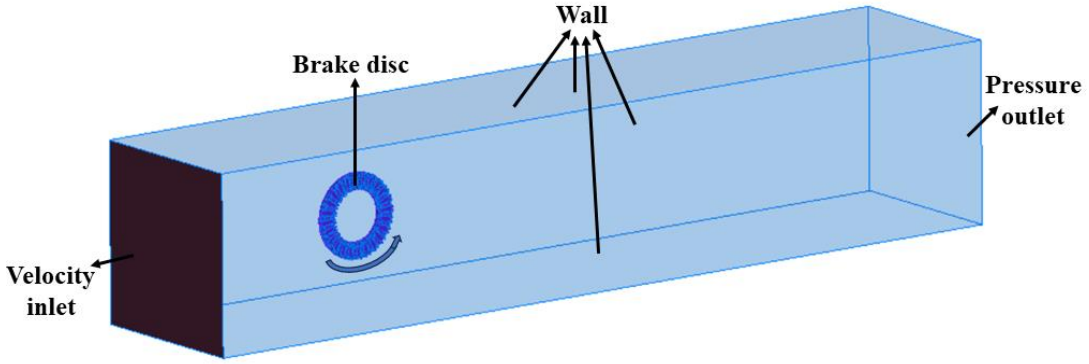

Fig. 4. Computational domain and boundary conditions

The brake disc solid rotates around the Z axis, and the angular speed of rotation is equal to that of the train axle. The ambient temperature of the solid surface of the brake disc and other walls and fluids is set to 300K, and the heat flux is applied to the friction surface of the brake disc. The heat flux is calculated as follows:

First, in order to simulate the emergency braking condition where the initial braking speed is 111.11m/s(400km/h), the train running speed during the emergency braking process changes as follows [2]:

$$\begin{cases} v(t) = 111.11 - 0.66t & (0 \le t \le 42.09) \\ v(t) = 83.33 - 1.07t & (42.09 < t \le 119.97) \end{cases}$$

Due to certain energy loss (wind resistance, brake disc vibration) during braking, not all kinetic energy is converted into heat energy, the energy conversion rate is 84%, and the converted heat energy is loaded to the friction surface in the form of heat flux. According to the fact that there are eight sets of wheel mounted brake disc systems, and the heat flow of the brake disc is assumed to be uniform on the friction surface.

$$q(t) = 0.84 \frac{d(\frac{1}{2}Mv_0^2 - \frac{1}{2}Mv^2(t))}{16Adt}$$

where M is the mass of the motor car and A is the friction surface.

3.2 Analysis of temperature distribution

Since friction heat is considered in the form of heat flux, it is more appropriate to use the average maximum temperature to describe the maximum temperature. The curves of the average maximum temperature $Tave\max$ of the bionic brake

disc under emergency braking over time are shown in Fig. 5, the T_{ave}max of Disc S, Disc P and Disc Z was 851.01℃, 829.13℃ and 813.73℃, which occurred at 90.4s, 90.5s and 89.2s, respectively. The temperature distribution changes with braking time, as shown in Fig. 6, the temperature distribution at the time of 30s, 90s and 120s shows that the highest temperature at any time appears on the friction surface, the temperature of the brake disc varies greatly along the thickness direction and also on the friction surface. Due to the shape difference of the heat dissipating rib, when the heat is transferred to the heat dissipation layer through the solid material, as the heat is continuously input to the disc surface, the heat conduction effect takes a certain time to work together to cause the above temperature difference. Through the experimental study on the relationship between brake disc damage and temperature, researchers found that the abnormal hot spot generated by emergency braking in the friction contact area of the brake disc is an important cause of thermal fatigue, oxidation and wear damage of the brake disc [6,7]. Temperature uniformity has an important impact on the reliability and life of the disc, therefore, it can be seen from the comparison of three bionic brake discs, the temperature distribution on the friction surface of Disc Z is more uniform, and the area of high temperature area within the same temperature range is smaller. The comparison results prove that the Disc Z bionic heat rib structure can achieve efficient heat transfer, which indicate that Disc Z has relatively good temperature equalization performance.

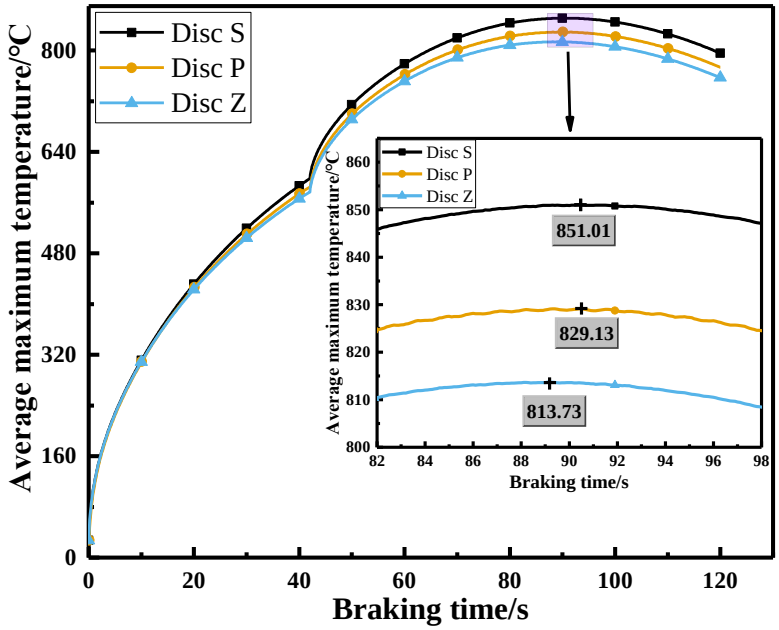

Fig. 5 Curve of average maximum temperature with time

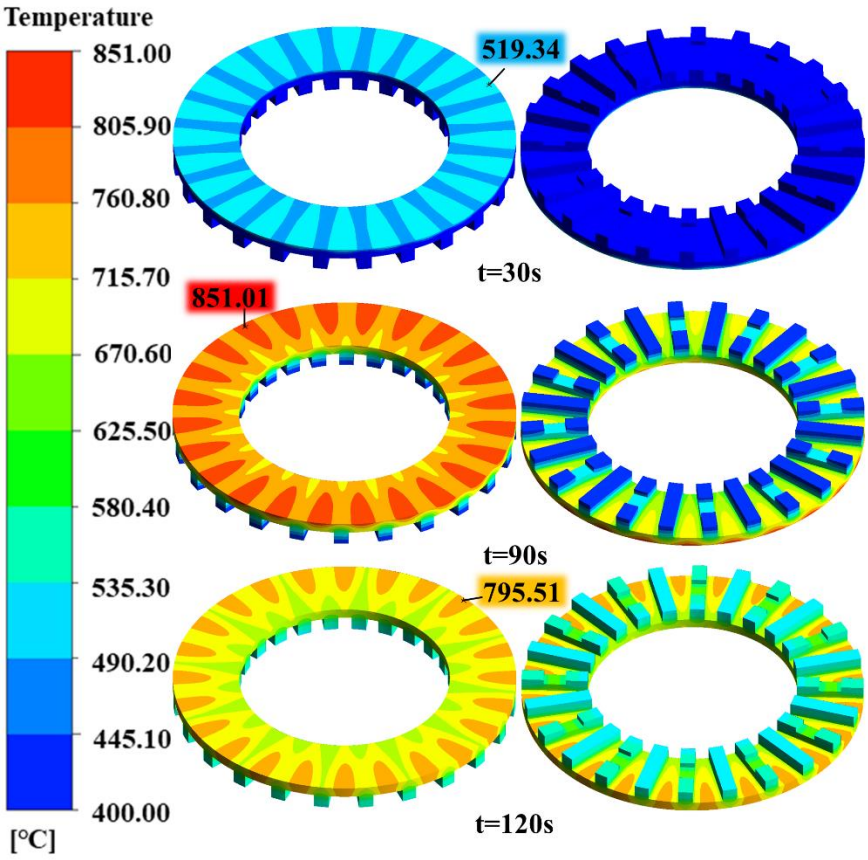

(a) Disc S

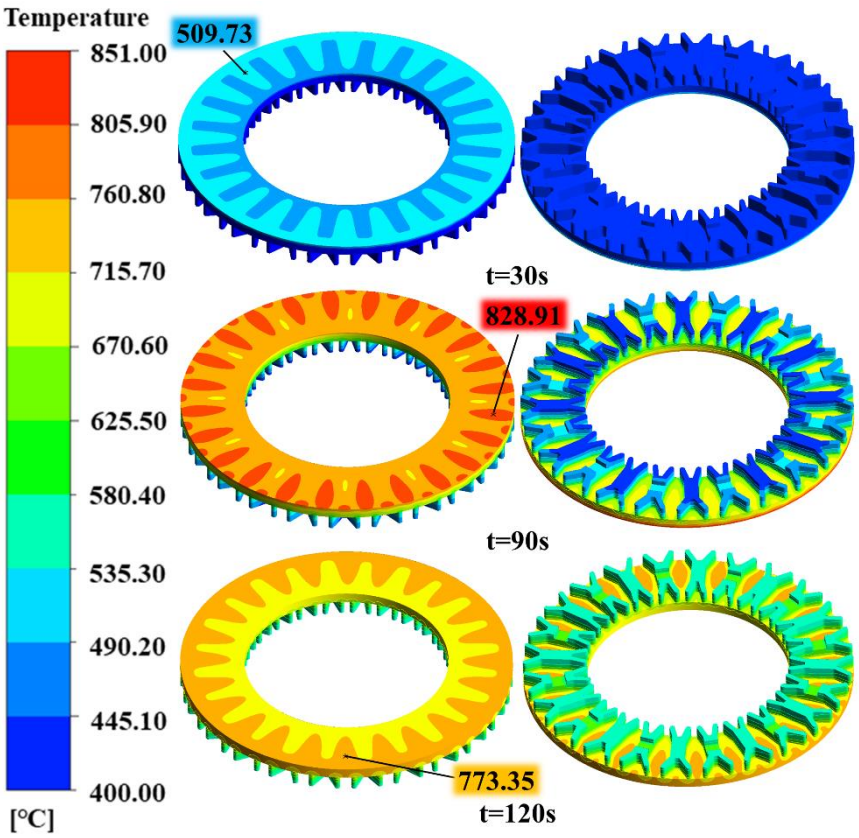

(b) Disc P

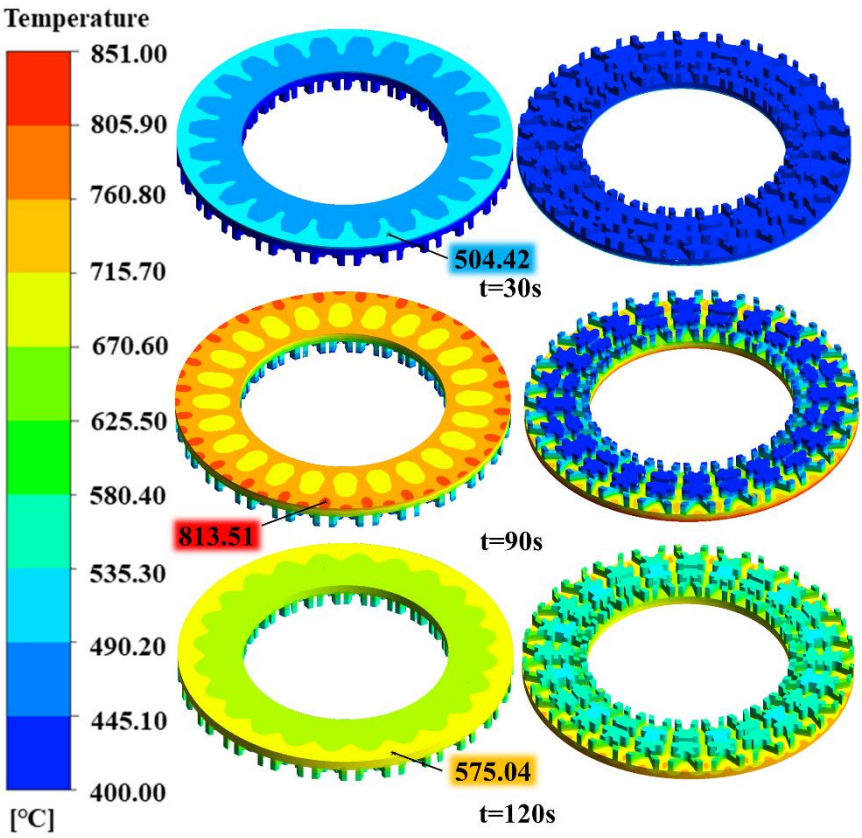

(c) Disc Z

Fig. 6. Temperature distribution of bionic brake disc

3.3 Analysis of aerothermal performance

Changing the material distribution of the heat dissipating rib can effectively improve the heat conduction process, reduce the maximum temperature value, and then reduce the thermal shock damage to the performance of the brake disc. In addition, there is a temperature difference between the solid and the surrounding air, which makes the flowing air carry away the heat of the disc surface, forming a convective heat transfer between the brake disc and the surrounding air, which also makes an important contribution to effectively preventing the performance of the disc from decreasing due to excessive temperature. This is because in the long-term heat dissipation process, heat convection heat transfer accounts for more than 90% of the three forms of heat dissipation: heat convection, heat conduction and heat radiation. Convective heat transfer coefficient is an important index to evaluate the convective heat transfer ability of the heat transfer structure, the convective heat transfer coefficient distribution is described in Fig. 7, it can be seen that Disc P and Disc Z structures have higher convective heat transfer coefficients, this is due to that compared to Disc S, Disc P and Disc Z have a staggered reinforcement structure, which controls the angle of air getting in and out of the heat fins, thereby improving the pumping effect of the brake disc. In addition, Disc Z has a wider regional distribution of high convective heat transfer coefficient than Disc P, which can be considered as the fractal rib not only increases

the heat transfer area, but also promotes the mixing of core fluid and boundary layer by disturbing the air around the brake disc, making the local heat exchange more sufficiently.

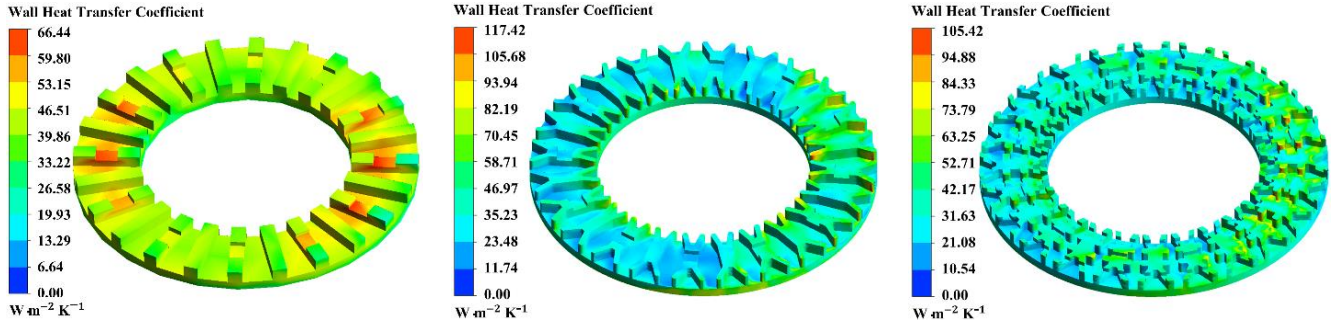

(a) Disc S (b) Disc P (c) Disc Z

Fig. 6. Convective heat transfer coefficient distribution of bionic brake disc

In order to compare the aerothermal characteristics of the bionic brake disc cooling rib, the convective heat transfer coefficient (h), the total heat transfer rate (Q_{rate}) and the average maximum temperature ($Tave\max$) are listed in Table 2. It can be seen from the table that the three bionic brake discs have similar h values, but the h of Disc P is relatively high, it is 40.46 $W \cdot m^{-2} \cdot K^{-1}$. According to the analysis of heat exchanger in reference [7], the total heat exchange is an important index to evaluate the heat transfer performance of the heat sink, total heat transfer is the sum of heat transfer to the surrounding air by each volume unit. When solving h, since the reference temperatures of fluid and solid of these discs are set to be equal, the total heat transfer rate is defined as:

$$Q_{rate} = \frac{Q_{total}}{T_0 - T_W} = h \bullet A_{surf}$$

Table 2 Comparison of aerodynamic thermal performance indexes of brake disc

Model	h ($W \cdot m^{-2} \cdot K^{-1}$)	Q_{rate} ($W \cdot K^{-1}$)	$Tave\max$ (°C)
Disc S	39.85	33.79	851.01
Disc P	40.46	38.43	829.13
Disc Z	38.16	39.19	813.73

4. Multi-objective optimization

4.1 Design variables

Literature research and the design concept of heat dissipating rib show that, for bionic Disc Z brake disc, the entrance angle φ, exit angle θ and the number of heat rib n are the main design parameters that affect the above thermal performance. The aerodynamic thermal performance of brake disc is improved by multi-objective optimization, according to the above analysis, parameters φ, θ and n are taken as optimization variables, and $Tave\max$ and h are taken as objectives function. The value range of variables is as Table 3.

Table 3 Design variables and level values

Variables	$\varphi(°)$	$\theta(°)$	$n(/)$
Lower	0	0	12
Upper	55	45	24

The Modified Extensible Lattice Sequence (MELS) DOE algorithm is chosen, this method spreads points equally in the many dimensional design space, avoiding clumps and empty spaces. 36 sample points are generated, which are shown in Fig. 8. the geometric model corresponding to the sample points is established by using NX12.0. then CFD software is used to solve the three-dimensional flow and heat transfer equations.

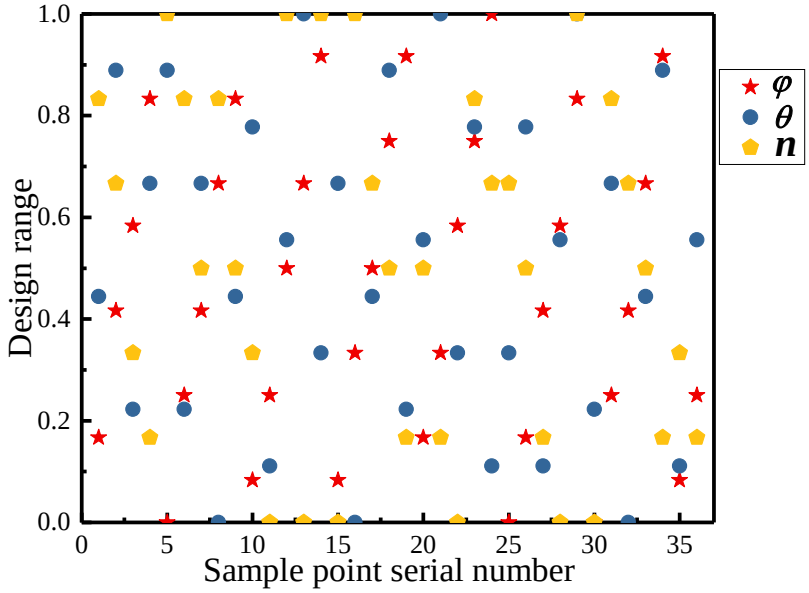

Fig. 8. Distribution of sample points generated by the modified extensible lattice sequence

4.2 Approximation model

Approximate models of design variables and responses need to be established in order to improve computational efficiency, when an approximate model is built to approximate the design variables and the response values, the amount of computation increases exponentially with the increase of the variables. Due to the limitation of the number of sample points. Least Squares Regression (LSR) minimizes the sum of squares of the response predicted by the regression model and the corresponding simulation model residuals by creating a regression polynomial of the selected order, i.e.

$$\min E = \sum_{i=1}^{n} (f_i^p - f_i)^2$$

Where n is the design number, f_i^p is the output response value of the i th design predicted by the regression model, and f_i is the output response value of

the i th design simulation. The coefficient value of the regression model is obtained by taking the derivative of E with respect to each unknown coefficient as 0. Interactive regression model is used to establish the polynomial associated with the response and variables. The regression model expressions of $Tave\max$ and h are as follows:

$$T_{ave\max} = 969.47 - 5.23n - 0.04\varphi \bullet n$$

$$h = -249.88 + 0.22\varphi + 0.58\theta + 0.06n^2 - 0.02\theta \bullet n$$

After the approximate model was established, it is also necessary to evaluate its prediction ability. The comparison between the calculation results and the predicted values of the approximate model is shown in Fig. 9. The coefficient of determination R^2 and the adjusted coefficient of determination R^2_adj are commonly used to evaluate the accuracy of the approximate model, as shown in Table 2. The R^2 and R^2_adj fitting responses of $Tave\max$ are 0.95 and 0.96, respectively, and the R^2 and R^2_adj fitting responses of h are 0.96 and 0.97, respectively, indicating that the approximate model has high accuracy.

Table 2 The coefficient of determination R^2 and adjusted coefficient of determination R^2_adj of the approximate model.

Predicted response	R^2	R^2_adj
$Tave\max$	0.95	0.96
h	0.96	0.97

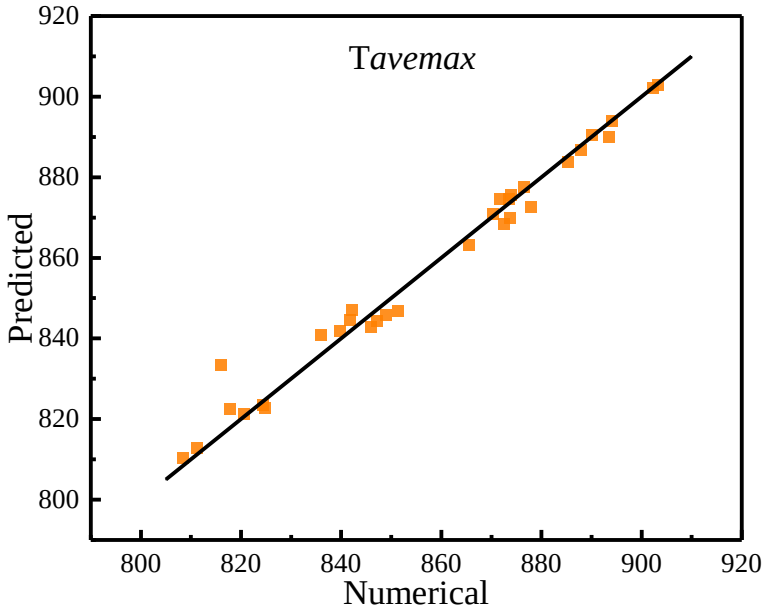

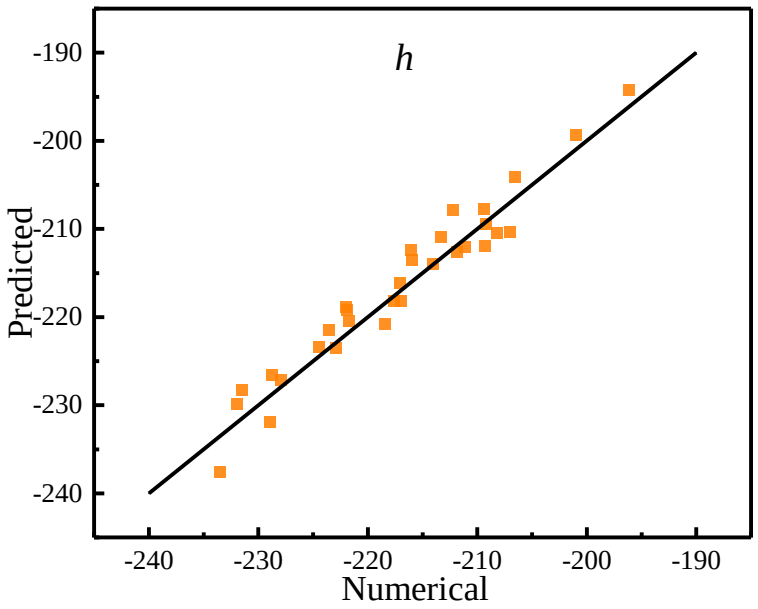

Fig. 9. Comparison of prediction results of the approximate model with CFD calculation results (a) $Tave\max$; (b) h .

4.3 Multi-objective optimization procedure

The design of brake disc with new materials needs to meet the dual requirements of high heat flux cooling capacity and enhanced heat dissipation. In order to obtain the optimal energy distribution design of the brake disc, two optimization objectives, the minimum average maximum temperature $Tave\max$ and the maximum convective heat transfer coefficient h after emergency braking of Disc Z brake disc, are used to carry out multi-objective optimization design. The multi-objective problem can be described as follows:

$$\begin{cases} Minmize & T_{ave\max}(\varphi,\theta,n) \\ Maxmize & h(\varphi,\theta,n) \\ Subject\ to & 0 \le \varphi \le 55 \\ & 0 \le \theta \le 45 \\ & 12 \le n \le 24 \end{cases}$$

The relationship between the response $Tave\max$ and h and the design variable is inconsistent, and it is difficult to meet the requirements of the two optimization objectives at the same time, so it is necessary to carry out multi-objective optimization of the two objectives. Multi-Objective Genetic Algorithm (MOGA) is adopted to approach the global Pareto-front. When there are multiple objective functions, the improvement of a single objective function is often accompanied by the reduction of another objective function, and multiple solutions will be generated. These solutions are called non-inferior solutions of the objective

function, i.e. Pareto optimal solutions. MOGA algorithm generates new individuals through crossover and mutation operations on selected individuals and adds them to the next generation population to promote genetic diversity, avoid prematurely falling into local optimal solutions, and use congestion distance measurement to evenly distribute Pareto frontier non-dominated points. The multi-objective optimization process is shown in Fig. 8. Firstly, based on the configuration characteristics and numerical results of the brake disc with optimal aerothermal performance, the optimization design variables and levels were determined. MSLS algorithm was used to determine the sample points in the design space. Using the LSR prediction model as the input function of MOGA, the Pareto optimal solution is obtained.

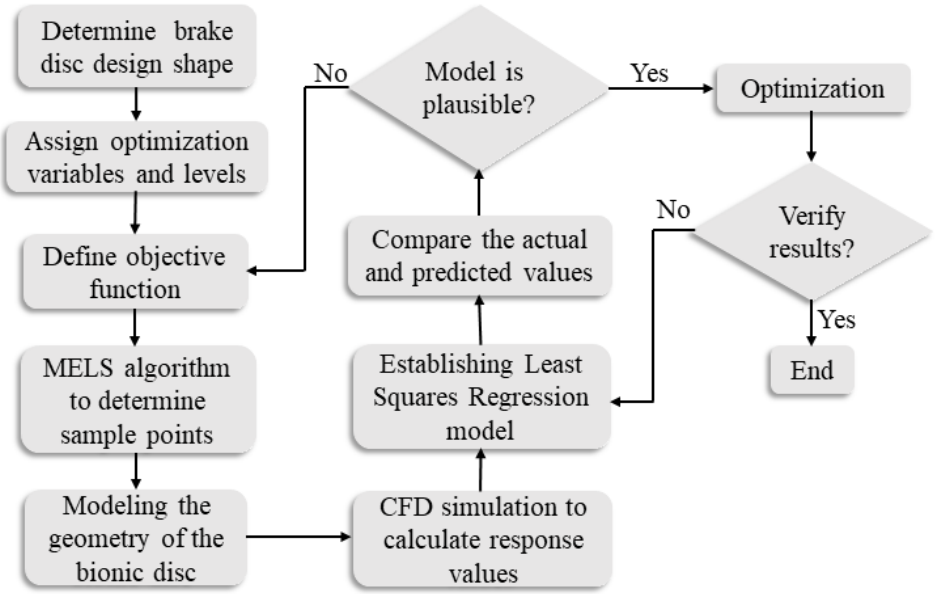

Fig. 8. Procedure for multi-objective optimization

4.4 Optimization result

The objective function obtains the Pareto frontier optimal solution after training, verification and testing, which contains 45 Pareto optimal designs (pods)(Fig. 9). The Pareto-optimal front curve represents all possible optimal tradeoff points between the conflicting objective functions $Tave\max$ and h, both of which are expressed in a minimized form where a higher $Tave\max$ is accompanied by a increase in the value of h. K-means clustering technique is used to select some iconic PODs to explain the change of the objective function with the change of the variable value. The variables and objective function values of the five different PODs are listed in Table 3. It can be seen from the table that POD1 has the smallest $Tave\max$ value, but also but the value of h is also the smallest.

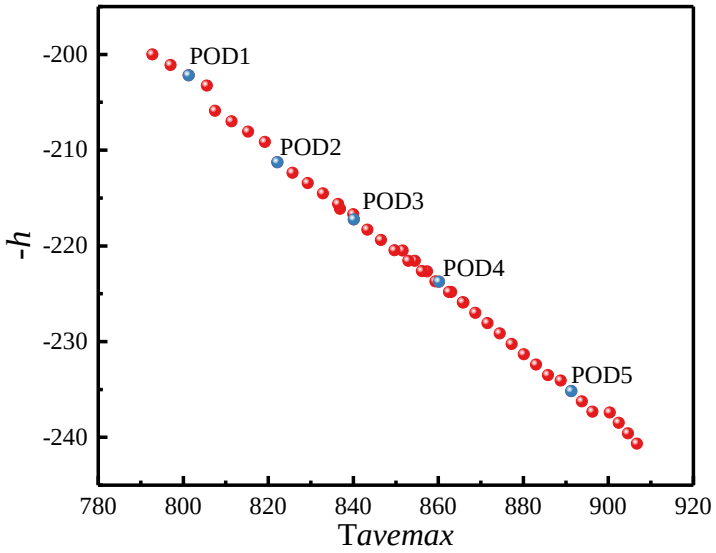

Fig. 9. Pareto-optimal front for the objective functions $Tave\max$ and h.

Table 3 Design variables and objective function values for representative PODs.

PODs	Design Variables			Objective functions	
	φ	θ	n	$Tave\max$	h
1	50	0	24	801.28	202.19
2	60	0	20	822.19	211.28
3	55	0	18	840.12	217.23
4	45	0	16	860.19	223.75
5	10	0	14	891.30	235.17

The T_{max} of POD1 is the smallest, but h is also the smallest, which means that the material distribution of POD1 is more reasonable, but the convective heat transfer capacity is poor, the T_{max} of POD5 is the largest, but h is also the largest, and the convective heat transfer capacity is the best. When moving from POD1 to POD5, the value of objective function T_{max} increases by 11.23% and the value of h decreases by 16.31%. The simulated T_{max}, h and Q_{rate} are listed in Table 4, and the total thermal performance of POD1 is the best, which is based on the premise that the use of lightweight carbon ceramic composite materials does not consider the impact of quality.

Table 4 numerical simulations of T_{max}, h and Q_{rate} for selected PODs

Model	T_{max} (℃)	h ($W\cdot m^{-2}\cdot K^{-1}$)	Q_{rate} ($W\cdot K^{-1}$)
POD1	801.06	202.76	213.51
POD2	818.11	204.22	206.67
POD3	836.76	215.03	207.50
POD4	857.76	226.97	208.81
POD5	893.17	232.13	198.00

Fig. 10 represents the comparison of predicted objective function values from optimization using those results which is obtained from numerical analysis for the illustrative PODs (POD 1–5). The MOGA predicted optimal values compared with the numerical simulations were found to be in excellent agreement with CFD, indicating a good generalization ability of the finalized PR models for the objective functions, T_{max} and h The maximum relative error was found to be 3.34% (POD 2) and 0.49(POD 2) for the objective functions, T_{max} and h respectively.

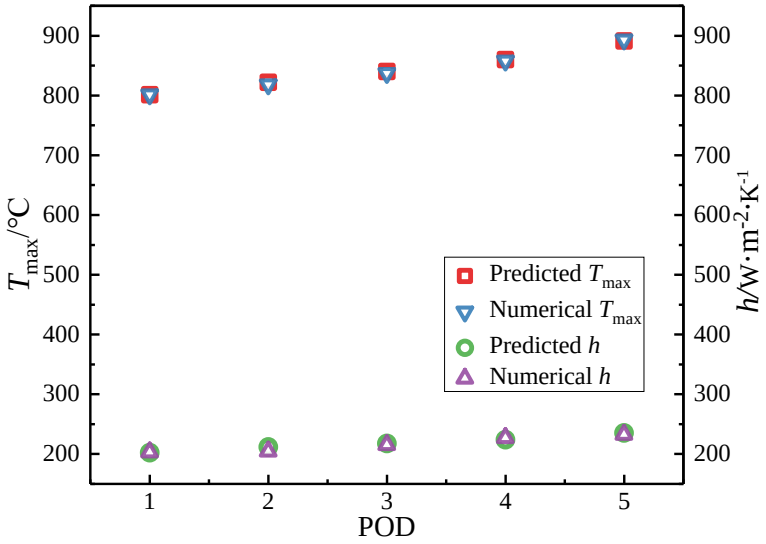

Fig. 10. Comparison between MOGA predictions and numerical simulations for selected PODs

Conclusion

The bionic concept of animal and plant nutrient delivery channel is applied to the thermal management of the brake disc, heat dissipating ribs of carbon ceramic composite are designed. In this way, the heat generated on the friction surface of the brake disc can be realized through heat conduction efficiently, and the convective heat transfer effect of the heat dissipating ribs is not weakened. Fluid-thermal coupling simulation was used to analyze the aerodynamic thermal performance of the brake disc under high-speed braking conditions, such as temperature, convective heat transfer and pressure drop. The comparison results showed that Disc Z had the lower maximum temperature (T_{max}), the higher total heat transfer rate (Q_{rate}), but also the higher pressure drop (Δp), which proved that the energy consumption of this structure was relatively high. However, the wind resistance energy consumption of brake disc relative to train body is almost negligible. Overall, the Disc Z showed relatively excellent aerothermal performance. To improve and control more efficiently the heat transfer mode of

the brake disc, the multi-objective optimization analysis is carried out. The inlet angle φ, outlet angle θ and number of heat dissipating rib n are selected as design variables, T_{max} and h of objective function are optimized. By constructing a MOGA model of the objective function, a pareto optimal frontier representing trade-offs between conflicting objectives is obtained in the function space of the design variables. The results show that the inlet angle and the number of heat ribs significantly affect the objective function. When the outlet angle is 0°, the aerodynamic thermal performance of the brake disc is the best. Without considering the influence of mass, the T_{max} and total heat transfer performance of POD1 are the best, this is as POD1 has enough materials to quickly release heat on the friction surface. In addition, the heat fin shape of POD1 have more convective heat transfer area. The maximum error of the prediction and numerical simulation results of the approximate model is 3.34% (POD 2) and 0.49% (POD 2), respectively, which shows the prediction effectiveness of the approximate model. In the optimization results, the outlet angle of 0° in the optimization results is consistent with the result that the temperature gradient distribution at the inner radius is more uniform, which is due to the material density at the inner radius is higher.

Acknowledgements

The research presented in this paper was conducted with the support of the National Key Research and Development Program of China (Grant No. 2021YFB3703801)

References

[1] Zmago Stadler,Kristoffer Krnel,Toma Kosma. Friction and wear of sintered metallic brake linings on a c/c-sic composite brake disc[J].Wear,2007,265(3):278-285.

[2] DUAN Junjie,ZHANG Menghang,CHEN Pengju,et al.Tribological behavior and applications of carbon fiber reinforced ceramic composites as high-performance frictional materials[J].Ceramics International,2021,47(14):19271-19281.

[3] Mori, H., M. Matsui and T. Tsujimura, Microstructural changes of A4340 steel brake discs due to thermal effects of running[J]. Iron and steel: The journal of the Society of Steelworkers of Japan, 2005. 91(12) 910-912.

[4] Yang Qiang. Simulation and Analysis of Train Brake Disc Temperature and

Stress Field[D]. Beijing, Beijing Jiaotong University, 2009.
[5] ZUO Jianyong,WANG Xueping,ZHOU Sufen,et al. Study on the applicability of thermal simulation method for brake discs of rolling stock[J]. China Railway Science,2022,43(5):78-86.
[6] Zhenzhong Wang, Research on crack expansion and microstructure evolution of brake disc friction surface of high-speed trains [D]. Beijing, Beijing Jiaotong University, 2020.
[7] Huang Xiaohua. Heat-machine coupling simulation analysis and structural optimisation design of brake discs for high-speed rolling stock[D]. Lanzhou:Lanzhou Jiaotong University,2019.
[8] Lv Xuemei. Structural Integrity Simulation of Carbon Fiber Composite Ceramic Brake Disc [D]. Beijing: Beijing Jiaotong University,2021.
[9] Fu Qiang. Thermal Coupling Analysis and Structural Optimization Design of Carbon Ceramic Moving Disc [D]. Jinan: Shandong University,2020.